nzsee
NEW ZEALAND SOCIETY FOR EARTHQUAKE ENGINEERING

Dynamic analysis of tall reinforced concrete walls designed with minimum vertical reinforcement

Tianhua Deng & Richard S. Henry
The University of Auckland, Auckland, New Zealand.

ABSTRACT

Analysis of tall walls subjected to earthquake ground motions highlights the amplified dynamic moment response at the mid-height due to higher mode responses. The amplified moment demand may result in unexpected reinforcement yielding outside of the plastic hinge region and impact termination rules for vertical reinforcement. The aim of this research was to investigate the dynamic response of tall reinforced concrete walls designed with minimum vertical reinforcement contents. A series of parametric analyses were conducted to investigate the effect of higher modes response on tall walls designed with light reinforcement contents, including the ground motion type and impact of cracking moment exceeding yield moment strength. An extreme case with higher concrete tensile strength, lower reinforcement contents at the upper stories, and lower axial load ratio was then conducted to investigate the impact of potential cracking and reinforcement yielding outside of the plastic hinge region. The dynamic analysis results showed no concentrated cracking or strain in the upper portion of taller walls that indicating the risk of premature fracture of reinforcement in the upper portion was low.

1 INTRODUCTION

Previous non-linear dynamic analysis of tall walls subjected to the earthquake ground motions highlights the amplified dynamic responses at the mid-height due to higher vibration modes. (Blakeley et al. 1975, Panagiotou and Restrepo 2009, Ghorbanirenani et al. 2012). The higher modes responses can lead to reinforcement yielding in the upper portion of walls (Filiatrault et al. 1994, Tremblay et al. 2001, Moehle et al. 2007), where the wall design only requires minimum distributed vertical reinforcement contents that are not intended to sustain inelastic flexural demands. Unexpected damage could occur within upper stories due to the flexural demands generated by higher mode effects and low section capacity caused by lightly reinforcement contents.

Recent studies have investigated the impact of vertical reinforcement content and layout on the ductility of the plastic hinge region of RC walls subjected to pseudo-static loading. The RC prism and wall tests

highlighted that the minimum distributed reinforcement in accordance with New Zealand design standards NZS 3101:2006 (A2) (2006) (~0.5% vertical reinforcement ratio) formed with the limited number of 1~3 primary flexural cracks resulted in the non-ductile failure (Patel et al. 2015; Lu et al. 2017). Other design standards have even lower minimum requirements (e.g. 0.25% for sections outside of the plastic hinge as per ACI 318-19 (ACI Committee 2019)), increasing the risk of non-ductile responses. The potential non-ductile response within the upper region in taller lightly reinforced walls would be exacerbated during dynamic loading as the higher modes amplify the moment demand at the mid-height.

The aim of the study was to investigate the potential damage pattern outside of the plastic hinge region for tall rectangular RC walls with minimum vertical reinforcement contents under earthquake excitation, as shown in Figure 1. A series of parametric analyses were conducted to investigate the higher modes effect on tall walls designed with light reinforcement contents, including the ground motion type, the impact of cracking moment exceeding yielding moment strength and the extreme case study with higher concrete tensile strength, lower reinforcement contents at the upper stories and lower axial load ratio.

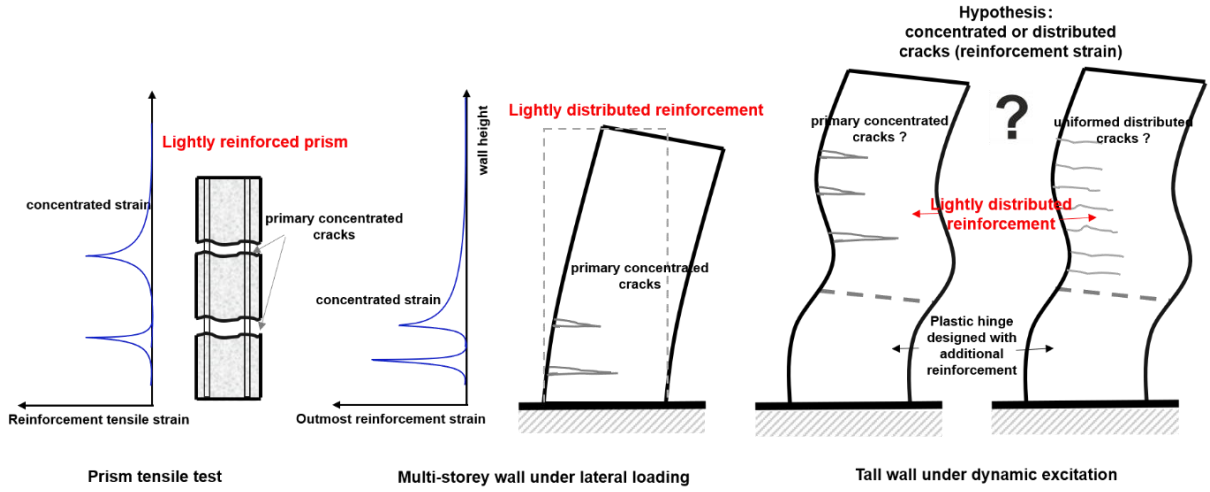

Figure 1: Crack distribution and strain response for lightly reinforced concrete members

2 MODEL DESCRIPTION

The developed model scheme that used a displacement-based element for the RC walls has been previously validated against tested walls with good accuracy in simulating both global and local responses when implementing the proposed regularisation techniques (Deng and Henry, 2022). For the fibre section in OpenSees, the modified Kent-Park concrete model available as Concrete02 (Yassin Mohd 1994) and Giuffré-Menegetto-Pinto steel hysteretic model (Menegotto and Pinto 1973; Filippou.F.C. et al. 1983) defined as Steel02 were used to capture the non-linear material responses.

2.1 Material properties

The compressive response of Concrete02 consists of three distinct regions, consisting of an ascending parabolic branch, a descending linear branch and a constant residual strength. The tensile response is defined by a bi-linear curve with zero residual strength after concrete cracking. The tensile strength was calculated in accordance with the fib Model code as $0.3(f_{ck})^{2/3}$, where f_{ck} is the characteristic compressive strength (fib Bulletin 65 2010), as shown in Figure 2a.

The Steel02 model consists of an initial slope E_s that is defined as the elastic modulus and a strain hardening slope expressed as bE_s, as shown in Figure 2b. The MinMax material command was coupled to define the

tension and compression ultimate strain limit in the stress-strain response, as shown in Figure 2c. Once the limits were triggered, the reinforcement stress immediately dropped to zero.

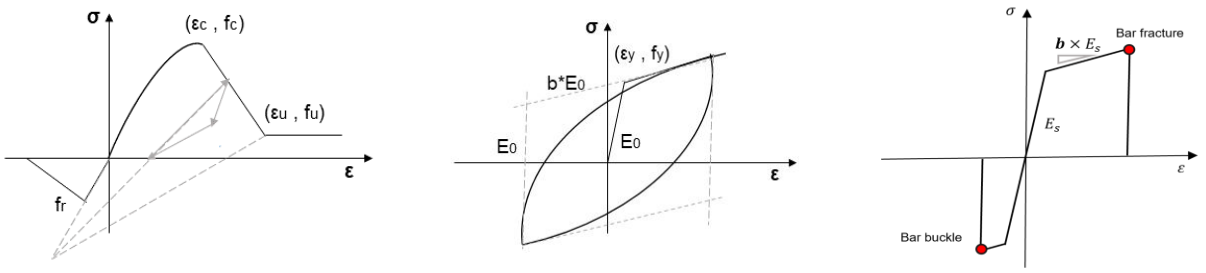

(a) Schematic Concrete02 stress-strain curve

(b) Schematic Steel02 stress-strain curve

(c) Integrate Steel02 with MinMax Command

Figure 2: Constitutive material models

2.2 Wall models

The wall model used to investigate the dynamic responses of tall walls was designed in accordance with ACI 318-19 (ACI Committee 2019). Key parameters were selected to investigate the impact of ground motion types, the exceedance of cracking moment than the yielding strength, and the extreme case with higher concrete tensile strength, lower reinforcement contents at the upper stories, and lower axial load ratio, which were summarized in Table 1.

The wall model was based on the web region of an existing 20-storey archetypical core wall model, with a thickness of 0.3 m, length of 8.2 m, storey height of 3.4 m, and the total height of 68 m (Panagiotou and Restrepo 2009), with the identical wall geometry and reinforcement arrangement, as shown in Figure 3. The walls were modelled with reinforcement Grade 60 with a yield strength of 420 MPa and ultimate strength of 620 MPa, as the recommendation in A615/A615M−18 (2018). The onset of reinforcement yielding and fracture strain was defined as 0.21% and 12%. The benchmark of tall wall model GM-std was designed according to the minimum reinforcement limits required for special structural walls in ACI 318-19. For the section within the plastic hinge region at the wall base, the minimum required vertical reinforcement ratio at the wall ends was 0.78% ($\sqrt{f_c'}/2f_y$), leading to two layers of 11 × D12.7 (#4) bars placed at 100 mm, and the required distributed minimum vertical reinforcement ratio in the web region was 0.25%, resulting in two layers of 32 × D9.5 (#3) bars placed at 200 mm centers, as shown in Figure 3 (a). For the section outside the plastic hinge region, the required distributed minimum vertical reinforcement ratio was 0.25%, resulting in two layers of 44 × D9.5 (#3) bars placed at 200 mm centers over the wall length, as shown in Figure 3 (b). For the model series of *cracking strength* and *extreme case*, the reinforcement ratio inside the plastic hinge region was adjusted in accordance with the concrete strength. The reinforcement ratio outside the plastic hinge region in *extreme case* series reduced to 0.15% that representing the lowest required vertical reinforcement in ACI 318-14 (2014). The seismic mass of 43,000 kg was imposed on the per storey that was satisfied with the prototype wall model (Panagiotou and Restrepo 2009), and the modelling damping in the study was defined as 3% with the consideration of non-linear response in high-rise buildings.

It should be noted that the minimum reinforcement requirements in ACI 318-19 (ACI Committee 2019) are less strict than in NZS 3101:2006 (A3) (New Zealand Standard 2017). Although ACI 318-19 requires that the same amount of reinforcement at the ends of the wall section within the plastic hinge as was adopted in NZS 3101:2006 (A3), the minimum required distributed reinforcement within the web region and outside the plastic hinge are lower in ACI 318-19.

Table 1: Details of the key parameters

Series	Wall No.	Base axial	Concrete compressive strength/ Cracking strength	Vertical reinforcement termination height	Reinforcement ratio inside plastic hinge region			Reinforcement ratio outside plastic hinge region
					End	Web	Total	
Ground motion type	GM-std	4%	40/3.5 MPa	5	0.79	0.25	0.40	0.25
Cracking strength	Post-C80-Cr6.3	1%	80/6.3 MPa	20	1.06	0.25	0.48	/
	Post-C80-Cr3.4	1%	80/3.4 MPa	20	1.06	0.25	0.48	/
Extreme case	Extreme-Dyn	1%	80/6.3 MPa	5	1.06	0.25	0.48	0.15

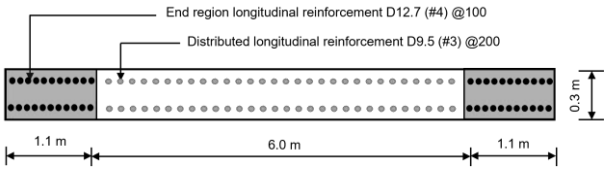

(a) Section details for the plastic hinge region at wall base

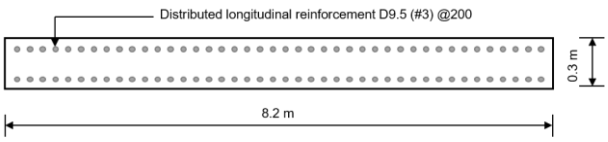

(b) Section details for outside plastic hinge region

Figure 3: Section details for the 20-storey RC tall wall

3 GROUND MOTION RECORDS

The impact of ground motion on the responses of taller lightly reinforced concrete walls was investigated using three typical ground motions, representing the near-fault with the large and small pluses and far-fault ground motions. All the ground motions records used during this study were sourced from the PEER Ground Motion Database (https://ngawest2.berkeley.edu/).

3.1 Ground motion selection

The seismic response of structures can be fundamentally different at sites affected by fault directivity and the distance from the fault rupture. The near-fault ground motion probably consists of a velocity pulse. An essential property of pulse-like ground motion is the period of the velocity pulse, denoted as T_p. The ratio of the pulse duration to the first mode period T_p/T_1 is the sensitive impact on the dynamic response of tall structures (Baker and Cornell 2008; Casey and Liel 2012). In this study, three typical ground motions present

the near-fault with the large and small pulses, and far-fault were selected to investigate the ground motion type effect on the lightly reinforced concrete tall walls. The selected ground motions used in the analysis are shown in Table 2.

Table 2: Summary of ground motions

Earthquake	Fault directivity	Years	M_w	Station	Mechanism	R_{rup} (m)	T_p (s)
Chi-Chi	near-fault large pulse	1999	7.6	TCU075	reverse	0.89	5.60
Loma Prieta	near-fault small pulse	1989	6.9	Gilroy Historic Bldg	reverse	10.97	1.35
Imperial Valley	far-fault	1978	6.5	Delta	strike slip	49.93	-

3.2 Ground motion scaling

The ground motion acceleration records were scaled to match the design-level seismic demand based on a 5% damped design spectrum. The spectral ordinates of $S_{DS} = 1.0g$ and $S_{D1} = 0.6g$ were used to estimate the maximum demands for Seismic Design Category D and site class D soil conditions (FEMA P695 2009). The resultant spectrum of each record was scaled to the design target spectrum with Mean Square Error (MSE) scaling procedure to minimize the difference between the target and recorder spectral acceleration. The scaled response spectra are presented in Figure 4. The identical scaled ground motions were used in the study to compare the objective responses of the parameter sensitivity, although the small discrepancy in elastic stiffness was caused by the different axial load, vertical reinforcement amount and concrete strength.

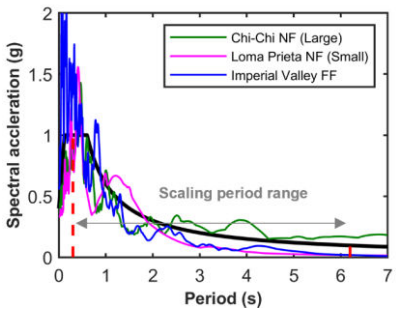

Figure 4: Section details for the 20-storey RC tall wall

4 ANALYSIS RESULTS

4.1 Impact of ground motion type

The model with a 4% axial load ratio was used to analyse the impact of ground motion type on the seismic response of tall walls. The modelled wall sections with an additional reinforcement height of 5 storeys in accordance with the minimum height required by ACI 318-19, as described in Table 1. Moment profiles that compare the pushover results at the maximum drift (green lines) and the maximum dynamic envelope (blue lines) with the calculated capacity (red lines) are shown in Figure 5 and strain profiles for the outmost tensile

reinforcement with the maximum strain values are shown in Figure 6. The strain profiles were consistent with the moment profiles with the reinforcement yielding where the dynamic demand exceeded the cracking strength. For the Chi-Chi earthquake representing the near-fault with large pulse ground motion, the peak strains were formed at the wall base and reinforcement termination height. While for the Loma Prieta earthquake with the near-fault with small pulse ground motion and the Imperial Valley earthquake with far-fault ground motion, a relatively pronounced "strain bulge" occurred at the upper stories. The dynamic moment and strain profiles were influenced by the ratio of the pulse period to the first mode period (T_p/T_1) that determined the dynamic responses (Baker and Cornell 2008; Casey and Liel 2012).

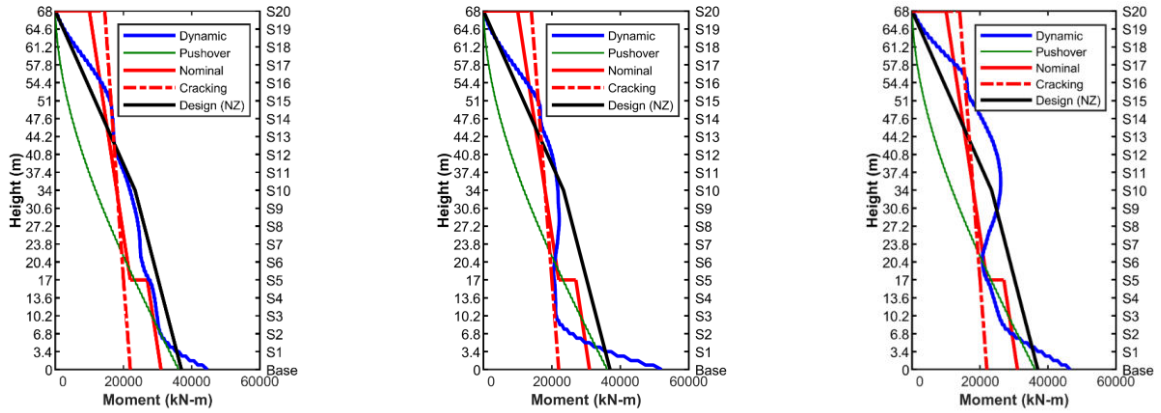

(a) Chi-Chi near-fault (large pulse)

(b) Loma Prieta near-fault (large pulse)

(c) Imperial Valley far fault

Figure 5: Comparison of the moment-response under different ground motion types

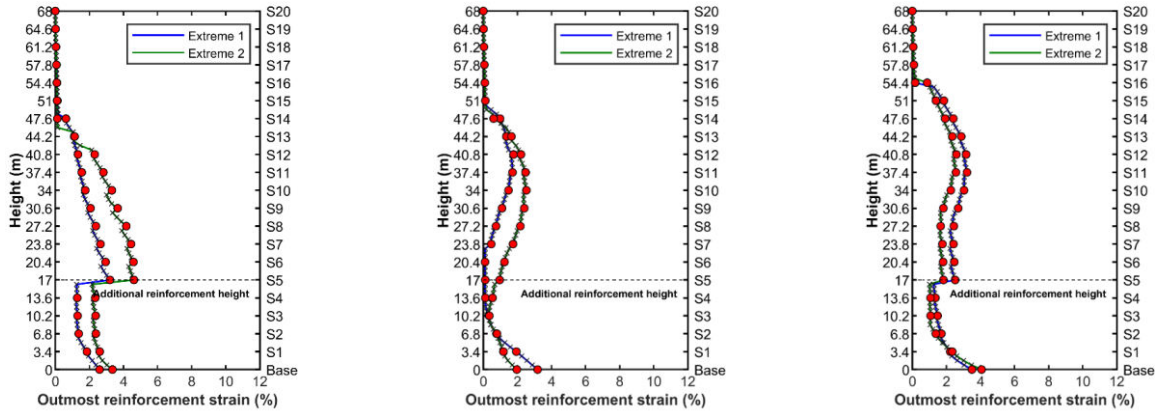

(a) Chi-Chi near-fault (large pulse)

(b) Loma Prieta near-fault (large pulse)

(c) Imperial Valley far fault

Figure 6: Comparison of the strain profile under different ground motion types

Table 3 compared the ratio of the pulse duration to the first mode period for the three ground motions. The tall walls under the Chi-Chi earthquake showed a larger period ratio than 1.0 ($T_p/T_1 = 1.03$) that indicates the first mode governs the wall responses so that the strain profiles were similar to the pushover result with the peak strain at the base and reinforcement termination height. The wall responses under the smaller period

ratio of Loma Prieta ($T_p/T_1 = 0.25$) and the far fault of Imperial Valley ground motions highlighted the larger moment and strain responses in the upper stories due to the pronounced higher modes response. It is worth noting that the required additional reinforcement height and upper reinforcement amount in ACI 318-19 would result in the maximum strain occurring outside the base detailed plastic hinge region.

Table 3: Comparison of the ratio of the pulse duration to the first mode period for three ground motions

Earthquake	Fault directivity	T_p (s)	T_1 (s)	T_p / T_1
Chi-Chi	near fault (large pulse)	5.60	5.44	1.03
Loma Prieta	near fault (small pulse)	1.35	5.44	0.25
Imperial Valley	far fault	-	5.44	-

4.2 Impact of cracking moment exceeding yielding moment strength

If the cracking strength exceeds the section yield strength, the rapid strength drop may result in a non-ductile response and sudden failure (Henry 2013; Lu et al. 2017). Post-cracking stiffness between the cracking and first yielding strength can be used to evaluate the proper force distribution in the reinforced concrete member (Bruun et al. 2020). Ensuring that the yielding strength exceeds the cracking strength is one criterion to achieve a ductile response and is defined as positive post-cracking stiffness, while a higher cracking strength causes a sudden failure with a limited number of cracks and is defined as negative post-cracking stiffness.

Two wall models were analyzed to investigate the impact of cracking stiffness on the seismic responses. The concrete tensile strength was defined as either 3.4 MPa and 6.3 MPa, which represented the lower and upper bound for concrete with compressive strength of 80 MPa in accordance with *fib* Bulletin 65 (2010). The models were designed with the same reinforcement content up the full wall height. The comparison of the section responses at the wall base and top in Figure 7 and Figure 8 showed the tensile stress of 6.3 MPa resulted in the negative post-cracking stiffness with a higher cracking strength than yield strength for model Post-C80-Cr6.3, and the lower tensile stress of 3.4 MPa led to the positive post cracking stiffness with a lower cracking strength than the yield strength for model Post-C80-Cr3.4. The comparison of the maximum moment profiles with the calculated design capacity envelops, and the maximum strain profiles for the outmost tensile reinforcement are shown in Figure 9 and Figure 10. Both models with different concrete tensile strengths showed the similar moment and strain responses, except at the several top stories where the higher concrete strength amplified the moment demands that resulted in a slightly higher yielding. The model results showed that walls with section cracking strengths that exceeded the yield strength would not experience worse damage as the higher cracking strength did not significantly impact the post-yield responses.

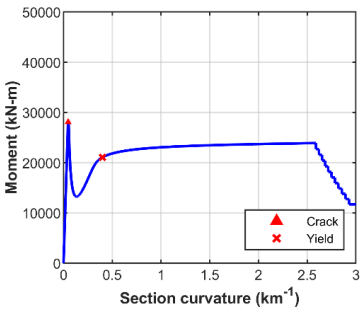

(a) Post-C80-Cr6.3 (6.3 MPa tensile stress)

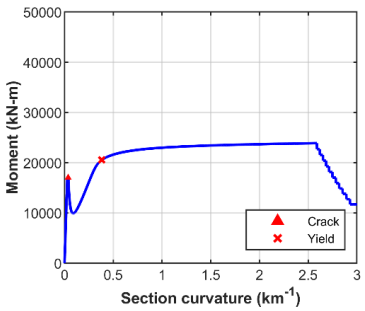

(b) Post-C80-Cr3.4 (3.4 MPa tensile stress)

Figure 7: Comparison of the base sectional capacity for different post-cracking stiffness

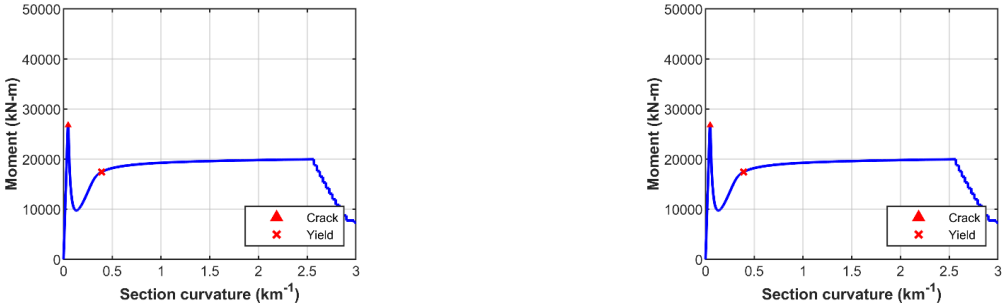

(a) Post-C80-Cr6.3 (6.3 MPa tensile stress) (b) Post-C80-Cr6.3 (3.4 MPa tensile stress)

Figure 8: Comparison of the top sectional capacity for different post-cracking stiffness

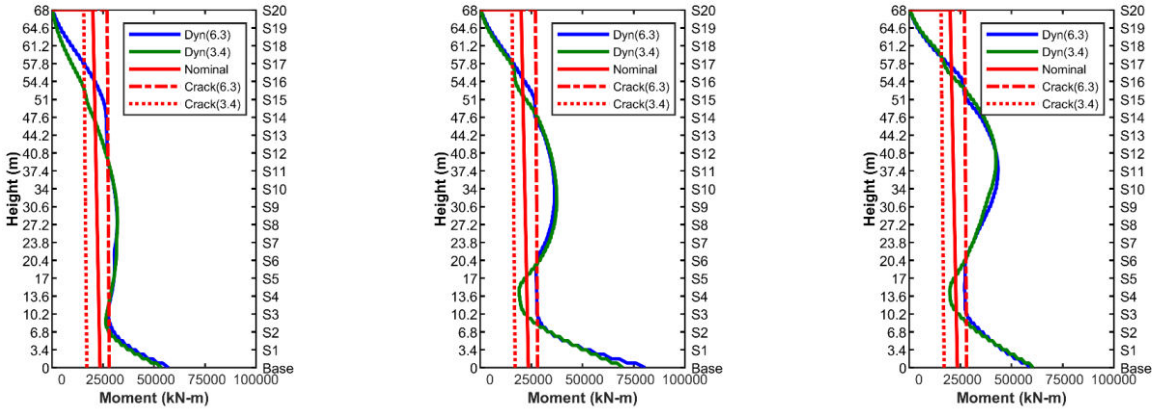

(a) Chi-Chi (b) Loma Prieta (c) Imperial Valley far fault

Figure 9: Comparison of the moment-response under different concrete tensile stress

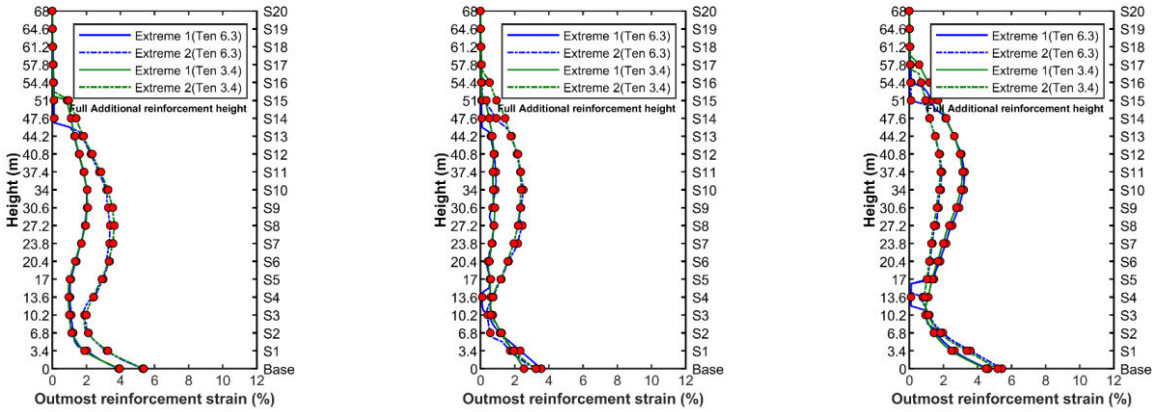

(a) Chi-Chi (b) Loma Prieta (c) Imperial Valley far fault

Figure 10: Comparison of the strain profile under different concrete tensile stress

4.3 Strain pattern in the wall portion

Prior pushover analyses of tall lightly reinforced concrete walls highlighted that insufficient reinforcement contents resulted in a peak strain at the reinforcement termination height (Deng and Henry, 2023). Due to the higher mode effects and low reinforcement content outside the detailed base region, it is essential to investigate the impact of potential cracking and reinforcement yielding in the upper stories of walls. The worst behaviour would occur with a combination of high concrete tensile strength of 6.3 MPa representing the upper bound of concrete with a compressive strength of 80 MPa (*fib* Bulletin 65 2010), low vertical reinforcement content of 0.15% for the upper storey in accordance with ACI 318-14 (2014), and low axial load ratio of 1% axial load representing the low gravity load to simulate the responses of lightly reinforced tall walls under the extreme case, as described in Table 1. The comparable peak moment and strain profiles under the three earthquake excitations are shown in Figure 11 and Figure 12. The section cracking strength (red dash line) exceeded the nominal strength (red solid line) up the entire wall height due to the combination of high concrete tensile strength, low vertical reinforcement content and low axial load. Due to the higher mode responses, the "bulge shaped" moment demand was amplified at the middle height. Compared with the concentrated moment at the base discrete sections in pushover analysis, the moment profiles were more gentle spread at the upper portion under the dynamic excitation resulted in a uniform strain profile.

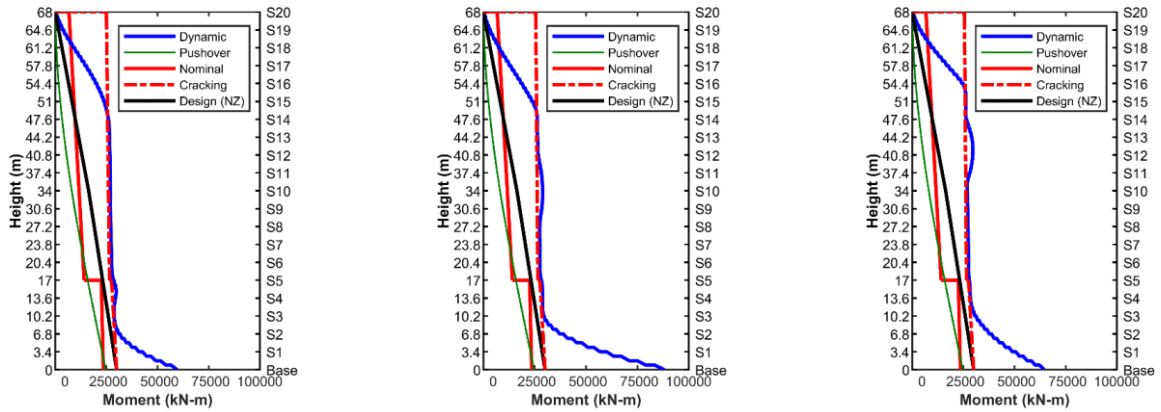

(a) Chi-Chi (b) Loma Prieta (c) Imperial Valley far fault

Figure 11: Comparison of the moment-response under combined extreme effects

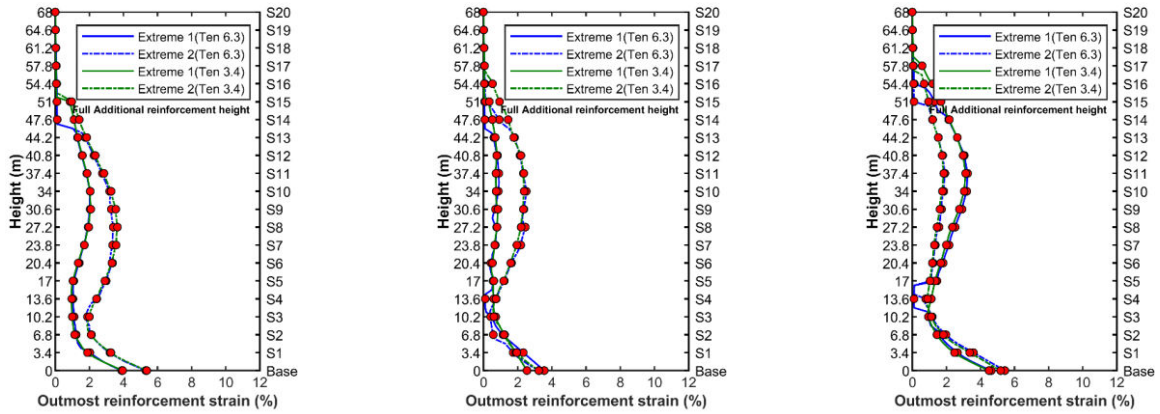

(a) Chi-Chi (b) Loma Prieta (c) Imperial Valley far fault

Figure 12: Comparison of the strain profile under combined extreme effects

The characteristic response for walls were the damage occurred at the wall base and in the upper portion are illustrated in Figure 13. For the lateral response of taller lightly reinforced walls where the cracking strength exceeds the nominal strength, the steep moment demand at the base results in the concentrated strain at a discrete number of cracks, as shown in Figure 13 (a). As the shaking wave travelled to the upper portion, the "bulge" shaped moment demand generated a more uniform strain response with distributed cracks when the moment demand exceeded the cracking capacity, as shown in Figure 13 (b). The model results of this extreme case indicate that despite the low reinforcement content, distributed cracks and a spread of reinforcement yielding develop in the upper region of tall walls when subjected to dynamic excitation. No analysis showed concentrated cracking or strains in the upper portion of the wall indicating the risk of premature fracture of reinforcement in the upper stories was low.

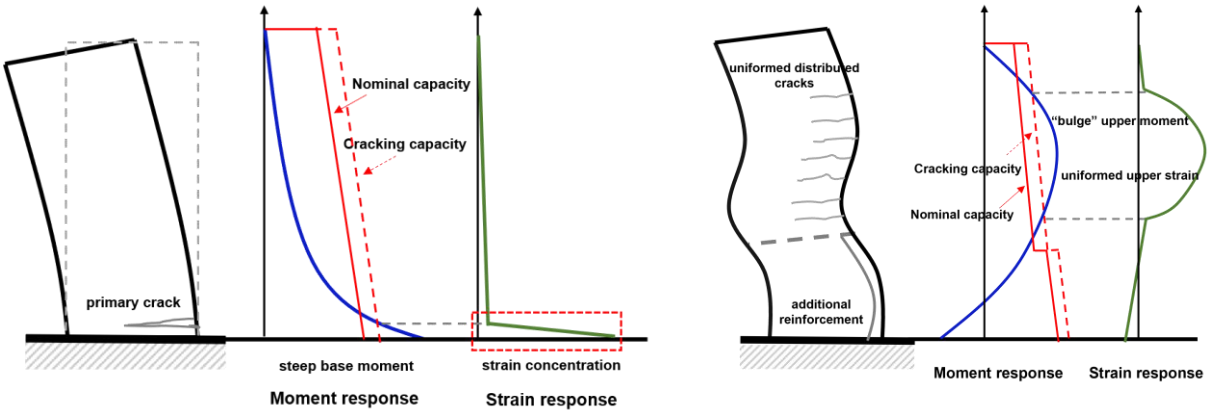

(a) Lightly reinforced concrete walls under lateral static loading

(b) Lightly reinforced concrete wall under dynamic loading

Figure 13: Illustration of the moment and strain response of lightly reinforced concrete walls

5 CONCLUSIONS

The dynamic responses of taller lightly reinforced concrete walls were investigated for the impact of ground motion type and cracking strength exceeding yielding strength, and strain pattern in upper portions. Preliminary findings from the numerical study are summarized as follows:

- The dynamic response for the upper portion of tall walls is significantly influenced by the ratio of the pulse period to the first mode period.
- Walls with higher section cracking strengths than the yield strength would not experience worse damage at the upper portion, as the concrete tensile strength has less impact on the dynamic moment and strain responses.
- Distributed cracks and a uniform yielding strain develop in the upper region of taller walls under dynamic excitation that is independent of vertical reinforcement content, concrete strength and axial load. No analysis showed concentrated strains in the upper portion of the wall that indicated the risk of premature fracture of the reinforcement in the upper stories was low.

6 ACKNOWLEDGEMENTS

The authors wish to acknowledge the Chinese Scholarship Council and the University of Auckland for providing financial support for this research program.

7 REFERENCES

A615/A615M−18. 2018. *Standard Specification for Deformed and Plain Carbon-Steel Bars for Concrete Reinforcement*. American Association State Highway and Transportation Officials Standard. https://doi.org/10.1520/A0615.

ACI 318-14. 2014. *Building Code Requirements for Structural Concrete(ACI 318-14)*. Vol. 11.

ACI Committee. 2019. *Building Code Requirements for Structural Concrete (ACI 318-19)*. American C. Michigan: Farmington Hills.

Baker, Jack W., and C. Allin Cornell. 2008. "Vector-Valued Intensity Measures for Pulse-like near-Fault Ground Motions." *Engineering Structures* 30 (4): 1048–57. https://doi.org/10.1016/j.engstruct.2007.07.009.

Blakeley, R.W.G, R.C. Cooney, and L.M. Negget. 1975. "Seismic Shear Loading At Flexural Capacity in Cantilever Wall Structures." *Bulletin of the New Zealand National Society for Earthquake Engineering* 8 (December).

Bruun, Edvard P.G., Allan Kuan, and Evan C. Bentz. 2020. "How to Model Post-Cracking Torsional Stiffness and Why It Matters in Design." *ACI Structural Journal* 344: 49–63.

Casey, Champion, and Abbie Liel. 2012. "The Effect of Near-Fault Directivity on Building Seismic Collapse Risk." *Earthquake Engineering & Structural Dynamics*, no. 41: 1391–1409. https://doi.org/10.1002/eqe.

Deng, Tianhua, and Richard Henry. 2022. "Regularisation Methods for Modelling Flexural Dominant Lightly Reinforced Concrete Walls." *Engineering Structures* 267 (June). https://doi.org/10.1016/j.engstruct.2022.114668.

Deng, Tianhua, and Richard Henry. 2023. "Investigation of Reinforcement Termination in Tall Lightly reinforced Concrete Structural Walls." *Structures*, Under review.

FEMA P695. 2009. "Quantification of Building Seismic Performance Factors." Washington, D.C.

fib Bulletin 65. 2010. *Fib Model Code 2010 Volume 1. The International Federation for Structural Concrete*

(Fib). Federal Institute of Technology Lausanne, EPFL

Filiatrault, A., D. D'Aronco, and R. Tinawi. 1994. "Seismic Shear Demand of Ductile Cantilever Walls: A Canadian Code Perspective." *Canadian Journal of Civil Engineering* 21 (3): 363–76. https://doi.org/10.1139/l94-039.

Filippou.F.C., Popov.E.P., and Beryero.V.V. 1983. *Effects of Bond Deterioration on Hysteretic Behavior of Reinforced Concrete Joints*. Earthquake Engineering Research Center, University of California,.

Ghorbanirenani, Iman, Robert Tremblay, Pierre Léger, and Martin Leclerc. 2012. "Shake Table Testing of Slender RC Shear Walls Subjected to Eastern North America Seismic Ground Motions." *Journal of Structural Engineering* 138 (12): 1515–29. https://doi.org/10.1061/(ASCE)ST.1943-541X.0000581.

Henry, R. S. 2013. "Assessment of Minimum Vertical Reinforcement Limits for RC Walls." *Bulletin of the New Zealand Society for Earthquake Engineering* 46 (2): 88–96.

Lu, Yiqiu, Richard S Henry, Ronald Gultom, and Quincy Ma. 2017. "Cyclic Testing of Reinforced Concrete Walls with Distributed Minimum Vertical Reinforcement." *Journal of Structural Engineering* 143 (5). https://doi.org/10.1061/(ASCE)ST.1943-541X.0001723.

Menegotto, Marco, and Paolo Emilio Pinto. 1973. "Method of Analysis for Cyclically Loaded R. C. Plane Frames Including Changes in Geometry and Non-Elastic Behavior of Elements under Combined Normal Force and Bending." *IABSE Reports of the Working Commissions*. https://doi.org/http://dx.doi.org/10.5169/seals-13741.

Moehle, Jack P;, Yousef; Bozorgnia;, and T.Y. Yang. 2007. "The Tall Buildings Initiative for Alternative." In *SEAOC 2007 Convention Proceedings*.

New Zealand Standard. 2006. *NZS 3101:2006-A2*. New Zealand Standards, Wellington, New Zealand.

New Zealand Standard. 2017. *NZS 3101:2006-A3*. New Zealand Standards, Wellington, New Zealand.

Panagiotou, Marios, and Jos´e I. Restrepo. 2009. "Dual-Plastic Hinge Design Concept for Reducing Higher-Mode Effects on High-Rise Cantilever Wall Buildings." *Earthquake Engineering & Structural Dynamics* 38: 1359–80. https://doi.org/10.1002/eqe.

Patel, V. J., B. C. Van, R. S. Henry, and G. C. Clifton. 2015. "Effect of Reinforcing Steel Bond on the Cracking Behaviour of Lightly Reinforced Concrete Members." *Construction and Building Materials* 96: 238–47. https://doi.org/10.1016/j.conbuildmat.2015.08.014.

Tremblay, R., P. Léger, and J. Tu. 2001. "Inelastic Seismic Response of Concrete Shear Walls Considering P-Delta Effects." *Canadian Journal of Civil Engineering* 28 (4): 640–55. https://doi.org/10.1139/cjce-28-4-640.

Yassin Mohd, Mohd Hisham. 1994. "Nonlinear Analysis of Prestressed Concrete Structures under Monotonic and Cyclic Loads." University of California, Berkeley. https://doi.org/10.16953/deusbed.74839.